2018 European Control Conference (ECC)
June 12-15, 2018. Limassol, Cyprus

Control oriented modeling of an electro-pneumatic gearbox actuator

Adam Szabo[1], Tamas Becsi[1], Peter Gaspar[2] and Szilard Aradi[1]

***Abstract*— The paper deals with the modeling of an electro-pneumatic gearbox actuator. The objective of the research is to develop the nonlinear, mathematical model of an electro-pneumatic gearbox actuator, which can be used as a Model in The Loop environment for controller testing purposes, and to derivate a simplified, multi-state, linear model, which will be the basis of controller development.**

I. INTRODUCTION

Pneumatic actuators use the compressed energy of the compressed gas to produce reciprocating linear motion and to achieve force transmission. A pneumatic actuator has lower specific weight and higher power density than an equivalent electro-mechanic actuator, and it is applicable on a wider temperature domain than the hydraulic actuators. Compressed air can be easily transported through tubes, it can be easily be stored, there is an unlimited supply of air to be compressed, while the exhausted air do not need to be collected, which means fluid return lines are unnecessary. Moreover they are easily maintainable, they have long life-time and high operational safety. Thus systems driven by pneumatic or electro-pneumatic actuators are widely used in industrial applications. A review of the industrial application of pneumatic systems can be found in [1]. They have a wide range of applications in the field of robotics, automation and manufacturing.

Since pneumatic muscle actuators (PMA) are one of the most promising actuators for applications that require greater proximity between humans and robots, a high number of recent studies focuses on the modeling and control of them, such as [2], [3] and [4]. While researches connected to the vehicle industry focus on the single- and double acting pneumatic cylinders. These are commonly used in systems, like exhaust gas recirculation, air brake systems [5], turbocharger applications [6], electro-pneumatic clutch [7], and gearbox actuator systems [8].

Against the many advantages of the electro-pneumatic systems, predicting their behavior and controlling them can be a complex task due to their nonlinear behavior. [9] One of the proposed methods is PID control, which should be enhanced through gain scheduling or it should be used in cascaded control [10]. Another control methods are the linear quadratic (LQ) control [8], which provides optimal control solution for a given cost function, the sliding mode control [11] and H-infinity method [12]. Further applicable controllers are the adaptive controllers [13], the fuzzy-based controllers [14] and the Neural Network based controllers, such as [15], [16] and [17].

The objective of the research is to develop the nonlinear, mathematical model of an electro-pneumatic gearbox actuator, which can be used as a Model in The Loop environment for controller testing purposes, and to derivate a simplified, multi-state, linear model, which will be the basis of controller development.

The paper is organized as follows: Section II describes the modeled actuator, Section III presents the development of the non-linear model. Section IV shows the model verification, and presents the simulation results compared to measurement results of the real system. Section V presents the derivation the state-space representation. Section VI shows some conclusion remarks.

II. SYSTEM DESCRIPTION

The modeled actuator is used for the automated manual transmission of heavy duty vehicles. Its function is to shift the proper gear inside a previously selected lane or to set the gearbox to neutral.

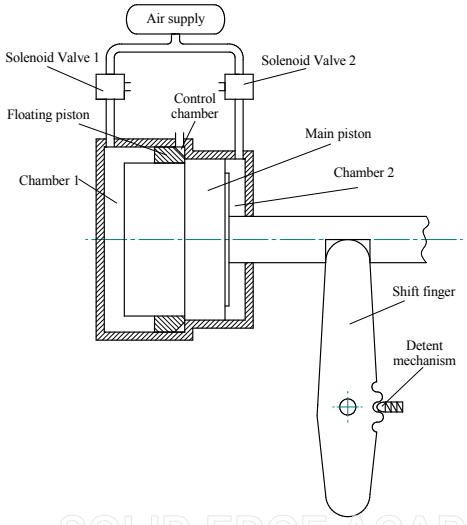

Fig. 1: Simplified layout of the gearbox actuator

*EFOP-3.6.3-VEKOP-16-2017-00001: Talent management in autonomous vehicle control technologies- The Project is supported by the Hungarian Government and co-financed by the European Social Fund

* The research is supported by the Magyar Automuszaki Felsooktatasert Alapitvany.

[1] Á. Szabó, T. Bécsi and Sz. Aradi are with the Department of Control for Transportation and Vehicle Systems, Budapest University of Technology and Economics, Stoczek u. 2, H-1111 Budapest, Hungary, [szabo.adam; aradi.szilard; becsi.tamas]@mail.bme.hu

[2] P. Gáspár is with the Systems and Control Laboratory, Computer and Automation Research Institute, Hungarian Academy of Sciences, Kende u. 13-17, H-1111 Budapest, Hungary gaspar.peter@sztaki.mta.hu

The pneumatic cylinder is driven by two 3-way 2-position solenoid valves. In energized state the solenoid valves connect the chambers to the supply pressure, while in released state they connect them to the ambient pressure. The layout of the modeled system can be seen in Fig. 1.

There are three chambers distinguished inside the cylinder: two working chambers and a control chamber. Both Chamber 1 and Chamber 2 are connected to a single solenoid valve which serves both input and output purposes, while the control chamber serves as an air spring with no solenoid valve connected to its only port.

In order to shift between different gears the main piston actuates the connected elements of the gearbox (such as the shift finger, and through it the synchronizer sleeve), therefore it has three dedicated positions: two gears (the High and Low end positions of the piston) and the Neutral position. Its movement is generated by the opposing pressure forces inside the working chambers. The function of the floating piston is to act against the movement of the main piston through collision and to tune the volume of the control chamber.

III. Nonlinear model of an electro-pneumatic actuator

The developed mathematical model is based on conservation equations such as the conservation of mass, energy and momentum. The system contains more than one element that shows hybrid behavior, therefore the equations describing the system change according to defined conditions. The dynamic model of the gear actuator essentially has three model parts: the solenoid valve model, the gear chamber model, and the model of the outer mechanisms.

The inputs of the models are solenoid valve commands and the force applied to the shift finger, while the modeled outputs are the pressures of the working chambers and the position of the main piston. Environmental and supply parameters are also the part of the system. The mathematical model of the solenoid vales can be found in related literature, such as [7] and [18].

A. Modeling assumptions and balance volumes

The deviation of the model should be as low as possible, but this would also mean high model complexity. While constructing the model the following assumptions were made in order to reduce model complexity:

1) The gas physical properties such as specific heats, gas constant and adiabatic exponent are assumed to be constant over the whole time, pressure and temperature domain.
2) The gas in the chamber is perfectly mixed, no spatial variation is considered.
3) Kinetic and potential energy of the gas is neglected.
4) The magnet valve elements are modeled assuming linear magneto-dynamically homogeneous material.
5) The cross sections of the solenoid valve ports are assumed to satisfy the following condition: $A_{MVout} >> A_{MVin}, A_{MVexh}$
6) The maximal stroke of the solenoid armature, inlet and exhaust ports are assumed to satisfy the inequality for the two valves: $x_{MVmax} > \frac{d_{MVinw}}{4} + \frac{d_{MVexh}}{4}$
7) All pressure forces are neglected on the solenoid valve armature.
8) Heat radiation is neglected and the rate of the heat exchange is proportional to the temperature difference between the gas and its surroundings
9) The masses of the pistons are assumed to be constant in time.

The dynamic equations of the actuator model are based on principles of predefined balance volumes. Since the gas in the chamber is assumed to be perfectly mixed, the model is lumped, thus the balances are ordinary differential equations. The balance volumes for the conservation equations are the following: Chamber 1, Chamber 2, Control chamber, Main piston, Floating piston and Shift finger balance volume.

B. Chamber thermodynamics

The gear chamber has two model parts: chamber thermodynamics and chamber mechanical dynamics. The applied conservation equations in the thermodynamical model are the conservation of mass and conservation of energy inside the chamber. In case of lumped parameter system the general expression for mass balance considering no generation and consumption terms can be written as the sum of the input and output mass flow rates of the system. Since both working chambers are loaded and unloaded through a sole 3/2 solenoid valve, the mass changes of the chambers are equal to the mass flow rate of the solenoid valves. Since there is no solenoid valve applied to the control chamber, the mass flow rate between the chamber and its environment is caused by the volume change of the chamber, which can be written as:

$$\frac{dm_{ch}}{dt} = A_{fl} p_1 \sqrt{\frac{2\kappa}{\kappa - 1} \frac{1}{R_{air} T_1} \left[(\pi)^{\frac{2}{\kappa}} - (\pi)^{\frac{\kappa+1}{\kappa}} \right]} \quad (1)$$

where A_{fl} is the area at vena contracta, κ is the heat capacity ratio, R_{air} is the gas constant for air, T_1 is the source side temperature, p_1 is the source side pressure and π is the pressure ratio, which can be determined as:

$$\pi = \begin{cases} \frac{p_2}{p_1}, & \text{if } \frac{p_2}{p_1} \geq \pi_{crit} \\ \pi_{crit}, & \text{if } \frac{p_2}{p_1} < \pi_{crit} \end{cases} \quad (2)$$

where p_2 is the counter side pressure,

The general form of total energy for a given balance volume with p input and q output flows is written as:

$$\begin{aligned} \frac{dE}{dt} = \sum_{j=0}^{p} \dot{m}_j^{in} (h + e_k + e_p) - \\ - \sum_{k=0}^{q} \dot{m}_k^{out} (h + e_k + e_p) + W + Q \end{aligned} \quad (3)$$

where h, e_k and e_p denotes the mass specific enthalpy, kinetic energy and potential energy terms respectively. Q is the heat transfer and W is the work term. Since the potential and

kinetic energy terms are neglected, the simplified energy balance equation applied to the chambers is written as:

$$\frac{dU_{ch}}{dt} = \dot{m}_{ch}h - W_{ch} - Q_{ch} \tag{4}$$

where U_{ch} is the internal energy of the gas. By expanding the terms in (4) the internal energy of the gas is the following:

$$\frac{dU_{ch}}{dt} = \dot{m}_{ch}c_pT_{inw} - p_{ch}\frac{dV_{ch}}{dt} - k_{ht}A_{ht}(T_{ch} - T_{amb}) \tag{5}$$

where c_p is the specific heat for constant pressure, T_{inw} is the temperature of the flowing air, V_{ch}, p_{ch} and T_{ch} are the volume, pressure and temperature of the chamber, k_{ht} and A_{ht} are the heat transfer coefficient and heat transfer area and T_{amb} is the ambient temperature.

$$\frac{dU_{ch}}{dt} = \frac{c_v}{R_{air}}p_{ch}\frac{dV_{ch}}{dt} + \frac{c_v}{R_{air}}V_{ch}\frac{dp_{ch}}{dt} \tag{6}$$

where c_v is the specific heat for constant volume. With the above introduced equations the chamber pressure gradient can be expressed as:

$$\frac{dp_{ch}}{dt} = \frac{\kappa_{air}R_{air}T_{inw}\dot{m}_{ch} - k_{ht}A_{ht}(T_{ch} - T_{amb})}{V_{ch}} - \\ - \frac{\kappa_{air}p_{ch}\frac{dV_{ch}}{dt}}{V_{ch}} \tag{7}$$

The volume of the chambers is given as the sum of cylinder and ring volumes with height taken from the axial displacement of the concerned elements, while the temperature of the chamber can be calculated according to the ideal gas law.

C. Chamber mechanical dynamics

The mechanical model of the actuator is based on the conservation equation for momentum. The applied momentum balance of the pistons can be written as:

$$\frac{dv_p}{dt} = \frac{\sum F_p - F_{cp} - F_{fp} + F_{fc} + F_{lim}}{m_p} \tag{8}$$

where F_p is the pressure force, which can be calculated from the pressures applied to the pistons. The second expression (F_{cp}) in (8) is the contact force between the pistons. This force only emerges if the two pistons collide and it is modeled as a stiff spring accompanied by a damping effect:

$$F_{cp} = \begin{cases} 0 \\ (x_{p1} - x_{p2})s_c + (v_{p1} - v_{p2})d_c \end{cases} \tag{9}$$

where x_{p1} and x_{p2} are the piston positions, s_c is the spring stiffness and d_c is the damping coefficient. The third (F_{fp}) and forth expressions (F_{fc}) in (8) are the friction forces. The applied friction model contains the Coulomb friction and the viscous friction. The switching characteristic of the Coulomb friction is approximated by a sigmoid-function. [19]

$$F_{coulomb} = F_\mu\left(\frac{2}{1 + e^{-f(v_1 - v_2)}} - 1\right) \tag{10}$$

where F_μ is the friction force between the elements, v_1 and v_2 are the speed of the friction elements and f is the gradient of the sigmoid function.

The last expression (F_{lim}) in (8) is the stroke limiting force. Upon reaching one of its end positions, the stroke limiting force is added to the piston. This force is only present when the piston stroke would exceed its limits and acts against the movement of the piston. It is modeled as the contact force between the pistons: a stiff spring accompanied by a damping effect:

$$F_{lim} = \begin{cases} (x_{pmin} - x_p)s_c - v_pd_c, & \text{if } x_p < x_{pmin} \\ (x_{pmax} - x_p)s_c - v_pd_c, & \text{if } x_p > x_{pmax} \\ 0, & \text{otherwise} \end{cases} \tag{11}$$

where x_{pmin} and x_{pmax} are the end positions of the piston.

D. Shift finger and detent mechanism

The mathematical model of the shift finger is based on the conservation of angular momentum. The shift finger works as a lever between the main piston and the synchronizer sleeve.

The conservation equation for the angular moment can be written as:

$$\frac{d\theta_{SF}\omega_{SF}}{dt} = F_cr_c - F_{ld}r_{ld} - tan(\alpha(x))F_{de}r_{de} \tag{12}$$

where θ_{SF} is the moment of inertia of the shift finger, ω_{SF} is the angular velocity of the shift finger, F_c and r_c are the contact force between the main piston and the shift finger, F_{ld} and r_{ld} are the force of the gear shift and its leverage, F_{de}, r_{de} and $\alpha(x)$ are the force of the detent mechanism, its leverage and the angle of the force. The contact force is modeled as it is shown in (9), the load force is the input of the simulation. The detent force passes through the rotation center of the shift finger, therefore it performs no torque on it, but assuming point like contact between the shift finger and the detent mechanism, the force can be expanded to a horizontal and a vertical component, which has moment on the shift finger.

IV. VERIFICATION AND VALIDATION

A. Verification

The model verification was performed by comparing the simulations to the real system behavior such as trends-, operation domain- and relationship of the variables. These attributes are gathered from multiple measurements and experiences of the actual system. During verification the environmental and supply parameters were assumed to be constant over time. The verified and validated outputs were the working chamber pressures and the main piston position.

In the verification and validation process four typical operating cases were considered, these are the following: from Neutral to High (Case 1), from High to Neutral (Case 2), from Neutral to Low (Case 3) and from Low to Neutral (Case 4) gear changes. An example of the first test case is shown on Fig. 2.

To move the main piston from Neutral to High position Solenoid Valve 1 is energized. It can be seen that after 3 ms delay the pressure in Chamber 1 starts increasing and after it reaches the value of the supply pressure it remains constant. When the pressure in Chamber 1 starts to increase there is

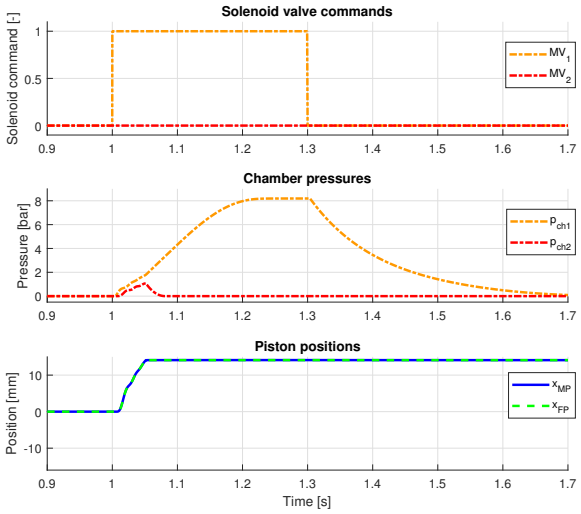

Fig. 2: Model verification

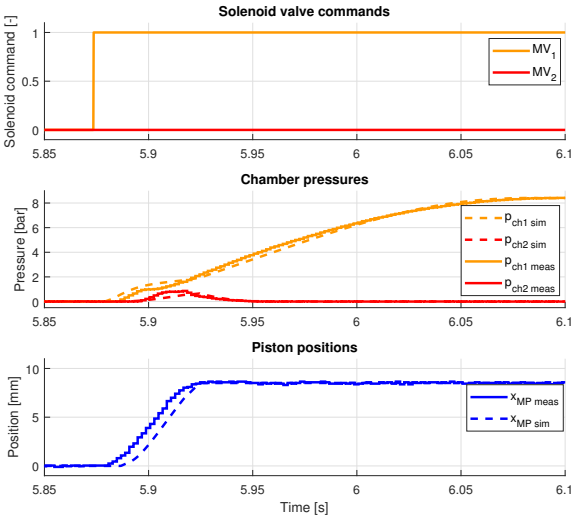

Fig. 3: Validation test case

also a 3 ms delay until the pressure force becomes high enough to move the piston. Upon reaching High position the movement of the main piston stops. Releasing the solenoid valve causes the pressure in Chamber 1 to decrease until it reaches the ambient pressure. While only Solenoid Valve 1 was energized, a small pressure increment can be seen in Chamber 2. This is caused by the sudden volume decrease inside Chamber 2 and the choke of the connected valve .

B. Validation

The developed model was validated against laboratory measurement, where the deviances of the simulation for each measured outputs were calculated with the following equation:

$$\epsilon^j_{y,i} = \frac{1}{T}\int_0^T \left(\frac{y^j_{i,meas}(t) - y^j_{i,sim}(t)}{y^{max}_{i,meas} - y^{min}_{i,meas}} \right) \tag{13}$$

All of the test cases were analyzed from the energizing of the solenoids until reaching the requested position. This granted that the constant states do not have effect on the calculated deviations. The validation was performed with the solenoid commands and the supply pressure imported from the measurement data, while there was no load force applied to the shift finger. The environmental and supply parameters were assumed to be constant over time, excluded the supply pressure. Since the used measurement data contains measurement errors, the unknown parameters (such as the discharge coefficients of the friction related parameters) were only estimated with heuristic methods.

The presented test case can be seen Fig. 3. The opening of the simulated solenoid valves is faster than the real one, since the simulated pressure of Chamber 1 starts to increase earlier, than the measured pressure. In spite of this, the simulated piston movement begins later, than it is in the measurement, but since the pressure difference between the measurement and the simulation is relatively small, the characteristic of the simulated piston movement is approximately equal to the measured one. The evaluation of the validation can be seen in Table I. It can be said that in Case 1 and Case 3, which are the more important test cases regarding the control of the actuator, the deviation of the simulation is within the accepted domain, while in Case 2 and Case 4 the deviation exceeds this domain, but the average deviation of the nonlinear model is acceptable.

TABLE I
MODEL DEVIATIONS

	E_{pch1} [%]	E_{pch2} [%]	E_{xmp} [%]
Case 1	4,29	2,1	4,5
Case 2	10,03	12,84	2,31
Case 3	3,37	7,36	6,82
Case 4	8,61	10,31	3,14
Average	6,58	8,15	4,19

V. STATE-SPACE REPRESENTATION

To control the nonlinear system with linear methods, a multi-state state-space representation of the modeled system is presented. Since the modeled system shows input-affine properties, the representation can take the following form:

$$\dot{\underline{x}} = \underline{f}(\underline{x}, \underline{d}, r) + \sum_{i=1}^{m} \underline{g}_i(\underline{x}, \underline{d}, r) u_i \tag{14}$$

$$\underline{y} = \underline{h}(\underline{x}, \underline{d}, \underline{u}, r) \tag{15}$$

The state matrices can be obtained by linearization, as it is shown:

$$\underline{\underline{A}} = \left.\frac{\partial \underline{f}(\underline{x}, \underline{d}, r)}{\partial \underline{x}}\right|_{\substack{x=x_0 \\ u=0}}, \ \underline{\underline{B}} = [\underline{g}_1, \underline{g}_2] \tag{16}$$

$$\underline{\underline{C}} = \left.\frac{\partial \underline{h}(\underline{x}, \underline{d}, \underline{u}, r)}{\partial \underline{x}}\right|_{\substack{x=x_0 \\ u=0}}, \ \underline{\underline{D}} = \left.\frac{\partial \underline{h}(\underline{x}, \underline{d}, \underline{u}, r)}{\partial \underline{u}}\right|_{x=x_0} \tag{17}$$

A. Further simplifications

For control design purposes the developed mathematical model has to be simplified. The model contains unmanageable number of hybrid states, therefore the reduction of these is required and the number of physical phenomenas also should be decreased.[18][20]

In the state-space representation the solenoid valve models are simplified and because of their small effect on the piston movement, the detent mechanism and the contact forces can be disregarded. The solenoid valve models are substituted with their mass flow rates, which can be calculated as the control chamber mass flow rate (see (1)), and the cross section area is a function of the solenoid command.

Disregarding the contact forces means, that the state-space representation cannot handle the collision between the pistons and the cylinder, and that the contact between the two pistons has to be taken into consideration in other ways. The function of the detent mechanism is to hold the pistons in the three dedicated positions if there is no actuation. Its effect against the pressure force is negligible. To decrease the computational cost of the state-space representation, the following simplifications are applied to the model.

Since the pressure change inside the control chamber is small during the actuations, it can be assumed to be equal to the ambient pressure.

The Coulomb-friction is a highly nonlinear element of the model, which could be used in the linearized model by deriving the sigmoid-function, but this method leads numeric errors, therefore it was handled as a constant and it is canceled out in the differentiation. The effect of the heat transfer is not significant inside the cylinder, therefore it can be left out of the simplified model.

Between Neutral and Low position only the main piston can move, in this case the floating piston can be neglected, while between Neutral and High position it is safe to assume, that the two pistons are moving together. This way the contact force between the pistons can be left out, since there is only one moving body, with position dependent mass.

B. Hybrid modes

With the shown simplifications the operation domain of the actuator can be described by two hybrid states, based on the position of the main piston and two hybrid states for each solenoid valves, based on their input signals. With the given simplification it is possible to reduce the number of hybrid states to eight and to reduce the number of state variables to four. The state vectors of the state-space representation are written as follows:

$$\underline{x} = \begin{bmatrix} p_{ch1} \\ p_{ch2} \\ x_{MP} \\ v_{MP} \end{bmatrix} \underline{y} = \begin{bmatrix} p_{ch1} \\ p_{ch2} \\ x_{MP} \end{bmatrix} \underline{u} = \begin{bmatrix} \dot{m}_{ch1} \\ \dot{m}_{ch2} \end{bmatrix} \underline{d} = \begin{bmatrix} p_{amb} \\ T_{amb} \\ p_{sup} \\ T_{sup} \end{bmatrix} \quad (18)$$

With the given state vectors, the state-space representation takes the following form, where $\underline{f}$, $\underline{g}_1$, $\underline{g}_2$ and $\underline{h}$ vectors are the function of $\underline{x}$, $\underline{d}$ and r:

$$\underline{f} = \begin{bmatrix} \frac{-\kappa_{air} p_{ch1} \dot{V}_{ch1}}{V_{ch1}} \\ \frac{-\kappa_{air} p_{ch2} \dot{V}_{ch2}}{V_{ch2}} \\ v_{MP} \\ \frac{\sum F_p - d_H v_{MP}}{m_{MP} + m_{FP}} \end{bmatrix}, \underline{h} = \begin{bmatrix} p_{ch1} \\ p_{ch2} \\ x_{MP} \end{bmatrix} \quad (19)$$

$$\underline{g}_1 = \begin{bmatrix} \frac{\kappa_{air} R_{air} T_{inw1}}{V_{ch1}} \\ 0 \\ 0 \\ 0 \end{bmatrix}, \underline{g}_2 = \begin{bmatrix} 0 \\ \frac{\kappa_{air} R_{air} T_{inw2}}{V_{ch2}} \\ 0 \\ 0 \end{bmatrix} \quad (20)$$

C. Example

As an example, the comparison of the State-Space model and the nonlinear dynamic model is made for a Low to Neutral gear change. Because of the switching behavior of the solenoid valves it shows only the energizing state of the valves. The related state matrices are the following:

$$\underline{\underline{A}} = \begin{bmatrix} a_{11} & 0 & a_{13} & a_{14} \\ 0 & a_{22} & a_{23} & a_{24} \\ 0 & 0 & 0 & 1 \\ a_{41} & a_{42} & 0 & a_{44} \end{bmatrix} \quad (21)$$

$$\underline{\underline{B}} = \begin{bmatrix} b_{11} & 0 \\ 0 & b_{22} \\ 0 & 0 \\ 0 & 0 \end{bmatrix}, \underline{\underline{C}} = \begin{bmatrix} 1 & 0 & 0 & 0 \\ 0 & 1 & 0 & 0 \\ 0 & 0 & 1 & 0 \end{bmatrix} \quad (22)$$

$$a_{11} = \frac{-\kappa_{air} A_{MP1} v_{MP}}{V_{ch1}} \quad (23)$$

$$a_{13} = \frac{-\kappa_{air} A_{MP1}^2 v_{MP} p_{ch1}}{V_{ch1}^2} \quad (24)$$

$$a_{14} = \frac{-\kappa_{air} A_{MP1} p_{ch1}}{V_{ch1}} \quad (25)$$

$$a_{22} = \frac{-\kappa_{air} A_{MP2} v_{MP}}{V_{ch2}} \quad (26)$$

$$a_{23} = \frac{-\kappa_{air} A_{MP2}^2 v_{MP} p_{ch2}}{V_{ch2}^2} \quad (27)$$

$$a_{24} = \frac{-\kappa_{air} A_{MP2} p_{ch2}}{V_{ch2}} \quad (28)$$

$$a_{41} = \frac{A_{MP1}}{m_{MP}}, a_{42} = \frac{-A_{MP2}}{m_{MP}}, a_{44} = \frac{-d_f}{m_M P} \quad (29)$$

$$b_{11} = \frac{\kappa_{air} R_{air} T_{sup}}{V_{ch1}}, b_{22} = \frac{\kappa_{air} R_{air} T_{sup}}{V_{ch2}} \quad (30)$$

The comparison of the two models in the given test case can be seen in Fig. 4. In case of the pressure of Chamber 2 there is no significant difference between the models, while in case of Chamber 1, the pressure calculated with the state-space realization is smaller, than the one simulated using the nonlinear model. In case of the state-space representation the piston movement is slower, than in case of the nonlinear model and it cannot reach Neutral position. This is caused by the absent of the Coulomb-friction. It can be seen, that the piston starts its movement earlier in the state-space model.

This means, that in the beginning of the gear change, the volume of Chamber 1 is bigger, compared to the nonlinear model. Since the mass flow rates are the same for the two models, this causes smaller pressure inside Chamber 1 in the state-space representation. Because of the smaller pressure, the actuating force is smaller, thus the piston velocity is significantly lower compared to the nonlinear model. This prevents the piston from reaching Neutral position.

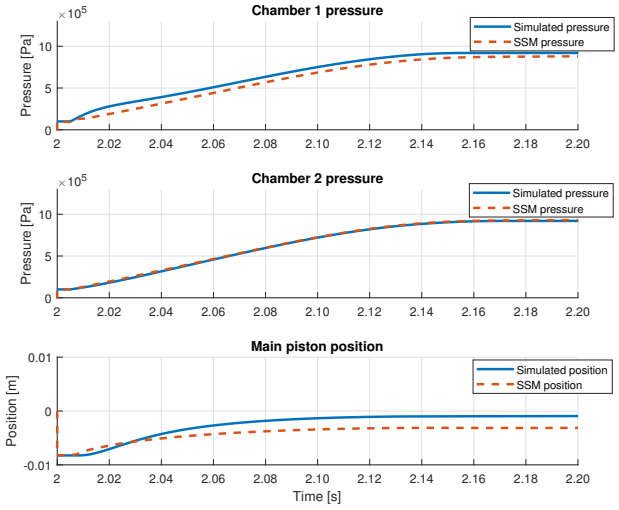

Fig. 4: Comparison of the nonlinear model and the state-space representation

VI. Conclusion and Future Work

The developed nonlinear model is capable of describing the dynamic behavior of the gearbox actuator, thus it can be used as a Model In the Loop environment for controller testing. Besides this, there is still room for further improvement of the system, such as for further parameter identification or for the implementation of a more detailed friction model.

The derived state-space representation is observable, controllable. The stability of the system is assured by the collision reaching the end positions and by the detent mechanism. The presented model describes the dynamic properties of the system properly, it can be used as a bases of controller development. However it is expectable, that additional modifications will be required, for instance the implementation of the Coulomb-friction.

Further research will focus on the development of a synchronizer model, which can be combined with the actuator model presented in this paper, and on the development of a cascade control loop for the combined model. This will be used to assure the position control of the actuator, while during synchronization it can reduce the stress appearing on the synchronizer elements.

References

[1] D. Saravanakumar, B. Mohan, and T. Muthuramalingam, "A review on recent research trends in servo pneumatic positioning systems," *Precision Engineering*, vol. 49, no. Supplement C, pp. 481 – 492, 2017.

[2] A. Hošovský, J. Piteľ, K. Židek, M. Tóthová, J. Sárosi, and L. Cveticanin, "Dynamic characterization and simulation of two-link soft robot arm with pneumatic muscles," *Mechanism and Machine Theory*, vol. 103, no. Supplement C, pp. 98 – 116, 2016.

[3] M. Oliver-Salazar, D. Szwedowicz-Wasik, A. Blanco-Ortega, F. Aguilar-Acevedo, and R. Ruiz-González, "Characterization of pneumatic muscles and their use for the position control of a mechatronic finger," *Mechatronics*, vol. 42, no. Supplement C, pp. 25 – 40, 2017.

[4] M. D. Doumit and S. Pardoel, "Dynamic contraction behaviour of pneumatic artificial muscle," *Mechanical Systems and Signal Processing*, vol. 91, no. Supplement C, pp. 93 – 110, 2017.

[5] P. Karthikeyan, C. S. Chaitanya, N. J. Raju, and S. C. Subramanian, "Modelling an electropneumatic brake system for commercial vehicles," *IET Electrical Systems in Transportation*, vol. 1, no. 1, pp. 41–48, March 2011.

[6] A. Mehmood, S. Laghrouche, and M. E. Bagdouri, "Modeling identification and simulation of pneumatic actuator for vgt system," *Sensors and Actuators A: Physical*, vol. 165, no. 2, pp. 367 – 378, 2011.

[7] B. Szimandl and H. Németh, "Dynamic hybrid model of an electro-pneumatic clutch system," *Mechatronics*, vol. 23, no. 1, pp. 21 – 36, 2013.

[8] ——, "Closed loop control of electro-pneumatic gearbox actuator," in *2009 European Control Conference (ECC)*, Aug 2009, pp. 2554–2559.

[9] E. Palomares, A. Nieto, A. Morales, J. Chicharro, and P. Pintado, "Dynamic behaviour of pneumatic linear actuators," *Mechatronics*, vol. 45, no. Supplement C, pp. 37 – 48, 2017.

[10] A. Saleem, B. Taha, T. Tutunji, and A. Al-Qaisia, "Identification and cascade control of servo-pneumatic system using particle swarm optimization," *Simulation Modelling Practice and Theory*, vol. 52, no. Supplement C, pp. 164 – 179, 2015.

[11] B. Szimandl and H. Németh, "Sliding mode position control of an electro-pneumatic clutch system," *IFAC Proceedings Volumes*, vol. 46, no. 2, pp. 707 – 712, 2013, 5th IFAC Symposium on System Structure and Control.

[12] ——, "Robust servo control design for an electro-pneumatic clutch system using the H∞; method," in *2014 IEEE/ASME 10th International Conference on Mechatronic and Embedded Systems and Applications (MESA)*, Sept 2014, pp. 1–6.

[13] Y.-T. Liu, T.-T. Kung, K.-M. Chang, and S.-Y. Chen, "Observer-based adaptive sliding mode control for pneumatic servo system," *Precision Engineering*, vol. 37, no. 3, pp. 522 – 530, 2013.

[14] T. Nuchkrua and T. Leephakpreeda, "Fuzzy self-tuning pid control of hydrogen-driven pneumatic artificial muscle actuator," *Journal of Bionic Engineering*, vol. 10, no. 3, pp. 329 – 340, 2013.

[15] N. N. Son, C. V. Kien, and H. P. H. Anh, "A novel adaptive feed-forward-pid controller of a scara parallel robot using pneumatic artificial muscle actuator based on neural network and modified differential evolution algorithm," *Robotics and Autonomous Systems*, vol. 96, no. Supplement C, pp. 65 – 80, 2017.

[16] C.-J. Chiang and Y.-C. Chen, "Neural network fuzzy sliding mode control of pneumatic muscle actuators," *Engineering Applications of Artificial Intelligence*, vol. 65, no. Supplement C, pp. 68 – 86, 2017.

[17] L. XiaoJun, Z. ChengRui, L. HongBin, and W. XinLiang, "Electronic pneumatic clutch control of the heavy truck based on neural network pid," in *2006 IEEE International Conference on Vehicular Electronics and Safety*, Dec 2006, pp. 232–235.

[18] H. Németh, L. Palkovics, and K. M. Hangos, "Unified model simplification procedure applied to a single protection valve," *Control Engineering Practice*, vol. 13, no. 3, pp. 315 – 326, 2005, aerospace IFAC 2002.

[19] F. Al-Bender, "Fundamentals of friction modeling," in *Proceedings, ASPE Spring Topical Meeting on Control of Precision Systems, MIT, April 11-13, 2010.* ASPE-The American Society of precision Engineering, 2010, pp. 117–122.

[20] B. Szimandl and H. Németh, "Systematic model simplification procedure applied to an electro- pneumatic clutch model," *Periodica Polytechnica Transportation Engineering*, vol. 43, no. 1, pp. 35–47, 2015.